

STEEP DECAY OF GRB X-RAY FLARES: THE RESULT OF ANISOTROPIC SYNCHROTRON RADIATION

Jin-Jun Geng^{1,2}, Yong-Feng Huang^{1,2}, Zi-Gao Dai^{1,2}

ABSTRACT

When an emitting spherical shell with a constant Lorentz factor turns off emission abruptly at some radius, its high-latitude emission would obey the relation of $\hat{\alpha}$ (the temporal index) = $2 + \hat{\beta}$ (the spectral index). However, this relation is violated by the X-ray flares in some gamma-ray bursts (GRBs), whose $\hat{\alpha}$ is much more steeper. We show that the synchrotron radiation should be anisotropic when the angular distribution of accelerated electrons has preferable orientation, and this anisotropy would naturally lead to a steeper decay for the high-latitude emission if the intrinsic emission is limb-brightened. We use this simple toy model to reproduce the temporal and spectral evolution of X-ray flares. We show that our model can well interpret the steep decay of the X-ray flares in the three GRBs selected as an example. Recent simulations on particle acceleration may support the specific anisotropic distribution of the electrons adopted in our work. Reversely, confirmation of the anisotropy in the radiation would provide meaningful clues to the details of electron acceleration in the emitting region.

Subject headings: gamma-ray burst: general — radiation mechanisms: non-thermal — relativistic processes

1. INTRODUCTION

For relativistic astrophysical phenomena, such as gamma-ray bursts (GRBs), it is known that the relativistic bulk motion would induce two significant effects on the radiation from their emission site when they are being observed. First, due to relativistic boosting, the emission is beamed in the direction of motion. So, for a jet with a certain opening angle (e.g., jets in GRBs or active galactic nuclei), the emission from higher latitudes will have a smaller Doppler factor. Second, due to the curvature of the geometry, photons at higher latitudes will arrive later than those from the line of sight although they are emitted simultaneously (Waxman 1997; Moderski et al. 2000; Granot 2005; Huang et al. 2007). The combination of these two effects is also called as the “curvature effect” for

¹School of Astronomy and Space Science, Nanjing University, Nanjing 210023, China, hyf@nju.edu.cn, gengjin-jun@gmail.com

²Key Laboratory of Modern Astronomy and Astrophysics (Nanjing University), Ministry of Education, Nanjing 210023, China

a relativistic spherical shell. In other words, for a long-lasting, spherical emitting jet, the photons received by the observer at specific observer time actually come from a distorted ellipsoid, rather than a spherical surface.

If the relativistic spherical shell flashes only at sometime, its temporal and spectral evolution of the light curve has been predicted by previous researches. Assuming the flux spectrum is a power-law form as $F_{\nu'} \propto \nu'^{-\hat{\beta}}$ in the co-moving frame of the shell and the bulk Lorentz factor of the shell Γ is a constant, then the observed spectral flux would obey $F_{\nu_{\text{obs}}}^{\text{obs}} \propto \nu_{\text{obs}}^{-\hat{\beta}} t_{\text{obs}}^{-\hat{\alpha}}$ and one can get the relation $\hat{\alpha} = \hat{\beta} + 2$ together (e.g., Kumar & Panaitescu 2000; Dermer 2004; Liang et al. 2006; Kumar & Zhang 2015), where ν' is the emitted frequency, ν_{obs} is the observed frequency, and $\hat{\alpha}$, $\hat{\beta}$ are the temporal index and spectral index respectively. Hereafter, the superscript prime (\prime) is used to denote the quantities in the co-moving frame and the letters “obs” is used to denote the quantities in the observer frame.

After the GRB trigger, X-ray flares are often observed, thanks to the the X-Ray Telescope (XRT; Burrows et al. 2005) on the *Swift* satellite (Gehrels et al. 2004). In general, X-ray flares show rapid rise and steep decay structures superposed on the underlying afterglow (Zhang et al. 2006). Several scenarios have been proposed for X-ray flares, including the clumpy accretion of the central engine (Perna et al. 2006), the reconnection-driven explosive event from a post-merger neutron star (Dai et al. 2006), the episodic accretion of the central black hole (Proga & Zhang 2006), or the delayed magnetic dissipation of the outflow (Giannios 2006), etc (see Kumar & Zhang 2015 for a review). Although the proper model for X-ray flares is still uncertain, some studies suggest that X-ray flares and the gamma-ray prompt emission may share a common origin, which further indicates that X-ray flares come from relativistic jets (e.g. Chincarini et al. 2007; Lazzati & Perna 2007; Maxham & Zhang 2009; Margutti et al. 2010). The X-ray flares may be released either by the dissipation of the magnetic energy (Mészáros & Rees 1997; Zhang & Yan 2011), or the kinetic energy of the jet (e.g. Paczynski 1986; Shemi & Piran 1990; Rees & Mészáros 1992). On the other hand, the decay phase of the X-ray flare should be the consequence of the cease of the energy release at the emitting site. Therefore, X-ray flares may be a well benchmark to test the curvature effect for a relativistic spherical shell.

Indeed, Uhm & Zhang (2015) have shown that the relation $\hat{\alpha} = \hat{\beta} + 2$ is invalid in the steep decay phase of some X-ray flares. Furthermore, they pointed out that this invalidation may be the evidence that the X-ray flare emission region is undergoing rapid bulk acceleration (Uhm & Zhang 2016; Jia et al. 2016). However, except for the bulk acceleration, there is another potential effect—the anisotropy of the radiation¹, that can change the standard relation. A main assumption above is that the radiation in the co-moving frame is isotropic, which still remains unconfirmed. If the radiation in the co-moving frame is anisotropic, i.e., the radiation is latitude dependent, then

¹ In this paper, by saying the anisotropy of the radiation, we mean that the emissivity of the emitting electrons would has anisotropic angular distribution averagely in the co-moving frame, rather than the anisotropic characteristics of jet’s properties (e.g., Dai & Gou 2001).

the decay phase would be determined by both the curvature effect and the intrinsic anisotropic characteristics. In fact, the steep decay induced by the anisotropy have been revealed in the afterglow (Beloborodov et al. 2011) and the prompt emission (Barniol Duran et al. 2016; Beniamini & Granot 2016; Granot 2016). One possible origin for the anisotropy is the preferable relative orientation between the direction of accelerated electrons and the magnetic field. Therefore, it is crucial to see whether the anisotropy can interpret the steep decay of the X-ray flares.

In our study, we select X-ray flares in three GRBs as example, of which the flare structures are clear and the data are of high quality. We show that the steep decay can be well explained by considering the anisotropy in the radiation. Our paper is organized as follows. In Section 2, we present the analytical derivation for the observed spectral flux in the case of anisotropic synchrotron emission. In Section 3, we develop a simple model to do numerical calculation and show how the anisotropy would reproduce the temporal and spectral evolution of these X-ray flares. The conclusions are summarized in Section 4.

2. RADIATION FROM A THIN SHELL

Like GRB’s prompt emission, X-ray flares are expected to be produced when the jet’s magnetic or kinetic energy is released. The emission region is far from the GRB central engine and can be treated as a part (limited opening angle) of an expanding spherical shell. Here, we take the synchrotron radiation as the main emission mechanism in X-ray flares and analytically derive the light curve from the shell. The spectral emissivity of a single electron of Lorentz factor γ_e at frequency ν' in the fluid rest frame is given by (Rybicki & Lightman 1979)

$$P'_{\nu'} = \frac{\sqrt{3}q_e^3 B' \sin \alpha}{m_e c^2} F\left(\frac{\nu'}{\nu'_c \sin \alpha}\right) = P'_0 \sin \alpha F\left(\frac{\nu'}{\nu'_c \sin \alpha}\right), \quad (1)$$

where q_e is electron charge, m_e is electron mass, c is the speed of light, α is the pitch angle between the direction of the electron’s velocity and the local rest frame magnetic field \mathbf{B}' , F is the synchrotron spectrum function², and $\nu'_c = 3q_e B' \gamma_e^2 / (4\pi m_e c)$. One can easily note that the term $\sin \alpha$ in Equation (1) indicates the dependence of the emissivity on α , which would further introduce the anisotropy in the radiation of a group of electrons as shown below.

For relativistic jets launched from the central rotating compact objects, the magnetic fields in them are expected to be mainly toroidal beyond the light cylinder (Lyubarsky 2009; Bromberg & Tchekhovskoy 2016). Also, the radial expansion of the jet would suppress the longitudinal component of the magnetic fields. So, in our modelling, we assume the magnetic fields \mathbf{B}' are transverse to the jet’s direction and they are tangled in the local shock plane. On the other hand, the electron distribution may be anisotropic, i.e., the angular distribution of electron moving

²The synchrotron spectrum function is defined as $F(x) = x \int_x^{+\infty} K_{5/3}(k) dk$, where $K_{5/3}(k)$ is the Bessel function.

directions is assumed to be described by a function $f(\alpha)$, which gives

$$\frac{dN_e}{d\Omega'_e} = N_{\text{tot}} \frac{f(\alpha)}{4\pi}, \quad (2)$$

where N_{tot} is the total number of the electrons and $f(\alpha)$ is normalized by $\int f(\alpha)d\Omega'_e = 4\pi$. By averaging $P'_{\nu'}$ on random B' in the shock plane, we can obtain the effective spectral emissivity per solid angle for a single electron as

$$\frac{d\bar{P}'_{\nu'}}{d\Omega'} \simeq \frac{A(\theta')}{4\pi} P'_0 F \left(\frac{\nu'}{\nu'_c A(\theta')} \right), \quad (3)$$

with

$$A(\theta') = \frac{1}{2\pi} \int_0^{2\pi} (1 - \sin^2 \theta' \cos^2 \phi)^{1/2} f[\arccos(\sin \theta' \cos \phi)] d\phi, \quad (4)$$

where θ' is the angle between the direction of emitted photons and the local radial direction and the geometric relation $\cos \alpha = \sin \theta' \cos \phi$ has been used. For approximation, the term $A(\theta')$ emerges in the coefficient and the spectral function F separately in Equation (3).

For a group of electrons which obey a spectrum of $dN_e/d\gamma_e$, the total spectral power from them should be

$$\frac{dP'_{\nu',\text{tot}}}{d\Omega'} = \int \frac{d\bar{P}'_{\nu'}}{d\Omega'} \frac{dN_e}{d\gamma_e} d\gamma_e \approx N_{\text{tot}} \frac{A(\theta')}{4\pi} P'_0 G \left(\frac{\nu'}{\nu'_c A(\theta')} \right). \quad (5)$$

In the last equality of Equation (5), we introduce the function $G(x)$ to approximate the integral of electron spectrum and to simplify the calculation. In practice, $G(x)$ should have a prior form according to the observations, such as a ‘‘Band-function’’ shape (Band et al. 1993).

2.1. Light Curve

We assume electrons in a spherical shell of radius r instantaneously emit photons in a very short time interval δt measured in the burst frame ($\delta t \ll \delta t_{\text{ring}}$, δt_{ring} is defined below). The shell is expanding with a bulk Lorentz factor Γ . An observer will first see photons emitted along the line of sight with $\theta = 0$ (θ denotes the latitude of the region on the shell). If we set the observer time t_{obs} equal to zero when receiving the photons emitted from $\theta = 0$, then photons from a location of θ will be detected by the observer at observer time

$$t_{\text{obs}} = \frac{r}{c}(1 - \mu)(1 + z), \quad (6)$$

where $\mu = \cos \theta$, and z is the redshift of the burst.

The number of electrons in the ring of $[\theta, \theta + \delta\theta]$ is $\delta\mu N_{\text{tot}}/2$ (N_{tot} is the total number of electrons of the shell). In the local burst frame, the specific spectral energy δE_{ν} emitted into the solid angle $\delta\Omega$ in δt can be related to the quantities in the co-moving frame by

$$\frac{\delta E_{\nu}}{\delta t \delta \Omega} = \frac{\mathcal{D}^2}{\Gamma} \frac{\delta E'_{\nu'}}{\delta t' \delta \Omega'} = \frac{\mathcal{D}^2}{\Gamma} \frac{dP'_{\nu',\text{tot}}}{d\Omega'}, \quad (7)$$

where $\mathcal{D} = \Gamma^{-1}(1 - \beta\mu)^{-1}$ is the Doppler factor. When the observer sees the ring, the corresponding energy is $\delta E_{\nu, \text{ring}} = \delta E_{\nu} \delta\mu/2$, the corresponding time duration is $\delta t_{\text{ring}} = r\delta\mu/c$. The spectral luminosity is thus $\delta L_{\nu} = \delta E_{\nu, \text{ring}}/\delta t_{\text{ring}}$. For an observer at distance D_L , the observed flux is $\delta F_{\nu_{\text{obs}}}^{\text{obs}} = \frac{(1+z)\delta L_{\nu}}{D_L^2 \delta\Omega}$, which can be further expressed as (also see Uhm & Zhang 2015)

$$\delta F_{\nu_{\text{obs}}}^{\text{obs}} = \frac{1+z}{4\pi D_L^2} \frac{c}{2r} \delta t \frac{A(\theta') N_{\text{tot}} P'_0 G((1+z)\mathcal{D}^{-1} A(\theta')^{-1} \nu_{\text{obs}}/\nu'_c)}{\Gamma^3(1 - \beta\mu)^2} \quad (8)$$

by combining Equations (5-7). Note that Equation (8) is only valid for the shell which flashes once (within δt), while it is analytically useful since we only focus on the steep decay phase here. When calculating the observed flux from a continually emitting shell, one should integrate the differential flux over the equal-arrival-time surface (Waxman 1997; Granot et al. 1999; Huang et al. 2000), or equally δt in Equation (8), which will be done in Section 3.

For $G(x) \propto x^{-\hat{\beta}}$, we can obtain

$$\delta F_{\nu_{\text{obs}}}^{\text{obs}} \propto A(\theta')^{1+\hat{\beta}} t_{\text{obs}}^{-(2+\hat{\beta})} \nu_{\text{obs}}^{-\hat{\beta}}, \quad (9)$$

where $A(\theta') = A(\theta'(t_{\text{obs}}))$ can be calculated by considering the relation $\cos\theta' = (\cos\theta - \beta)/(1 - \beta\cos\theta)$ and Equation (6). One can find that the flux is affected by the factor $A(\theta'(t_{\text{obs}}))$, which is further determined by the function f .

2.2. Anisotropic Case

In isotropic case, $A(\theta') = 1$, Equation (9) can recover the relation $\hat{\alpha} = 2 + \hat{\beta}$. However, for anisotropic case, the relation will not hold. Here, for instance, we consider the limb-brightened case, i.e., the emission is strong at $\theta' = \pi/2$ and weak near $\theta' = 0$. For photons emitted at $\theta' = \pi/2$, the angle between these photons and the radial direction in the observer frame is $\sim 1/\Gamma$. Therefore, most of the emission comes from a ring of angle $\theta = \Gamma^{-1}$ and the peak will be delayed comparing with the isotropic source (Barniol Duran et al. 2016).

On the other hand, if we assume $A(\theta') \propto (\sin\theta')^n$, $n > 0$, then using $\cos\theta' \simeq (\tau - t_{\text{obs}})/(\tau + t_{\text{obs}})$, we have

$$\delta F_{\nu_{\text{obs}}}^{\text{obs}} \propto \left[\frac{4\tau t_{\text{obs}}}{(\tau + t_{\text{obs}})^2} \right]^{(1+\hat{\beta})n/2} t_{\text{obs}}^{-(2+\hat{\beta})}, \quad (10)$$

where $\tau = r(1+z)/(2\Gamma^2 c)$, and $\beta \simeq 1 - \frac{1}{2\Gamma^2}$ is used. We will have the temporal decay index as

$$\lambda = -\frac{d \ln F_{\nu_{\text{obs}}}^{\text{obs}}}{d \ln t_{\text{obs}}} \simeq (1 + \hat{\beta})n/2 + (2 + \hat{\beta}), \quad (11)$$

where $t_{\text{obs}} \gg \tau$ is used. According to Equation (11), the anisotropy of the radiation will lead to a steep decay.

3. APPLICATION TO X-RAY FLARES

Based on the analysis above, we now propose a simple model and perform numerical calculations to reproduce the temporal and spectral behaviors of the X-ray flares. In order to achieve the steep decay, we choose a function f which corresponds to a limb-brightened case, i.e., $f(\alpha) \propto (a^2 + \sin^2 \alpha)^{-3}$, where a is the characteristic beaming angle of the electron distribution. This expression can be achieved when the electrons are preferentially moving along \mathbf{B} and the resulting expression for $A(\theta')$ is limb-brightened.

To perform the calculations, we need to notice the “timing” of the data of X-ray flares. Looking at the X-ray light curve, one may find one point ($t_{\text{obs}} = T_0$) after which the rising phase of the flare emerges. If we reset the reference time ($t_{\text{obs}} = 0$) at time T_0 , then the burst-frame time t can be connected to the observer-frame time t_{obs} by

$$t_{\text{obs}} = \frac{1}{c}[r_s + c(t - t_s) - r \cos \theta](1 + z), \quad (12)$$

where the initial photons of the flare are emitted at r_s at t_s , and $t = t_s + \int_{r_s} dr/(c\beta)$. However, the true value of T_0 may be obscured by the prompt emission and its precision is limited by the timing resolution of the observation. In practice, we use another parameter ΔT to describe the missed portion as is done in Uhm & Zhang (2015), so that the observer time of the flare is

$$t_{\text{obs}} = \frac{1}{c}[r_s + c(t - t_s) - r \cos \theta](1 + z) - \Delta T. \quad (13)$$

Moreover, the shape of the spectrum $G(x)$ should be given since we do not focus on detailed radiation mechanism in this paper. The spectrum of prompt emission is usually describe as a “Band” function (Band et al. 1993). However, the rapid softening of the spectrum during the decay phase of the X-ray flare indicates that the spectrum may be a power-law with an exponential cutoff (also see Uhm & Zhang 2016). We thus take $G(x) = x^{\zeta+1}e^{-x}$ in the following calculations.

In the co-moving frame, the total number of radiating electrons in the shell is $N_{\text{shell}} = 0$ at the starting radius r_s , and is assumed to increase at a rate R_{inj} before the turn-off radius r_{off} . In our calculations, we model the evolution of the characteristic Lorentz factor γ_{ch} , and R_{inj} as

$$\gamma_{\text{ch}}(r) = \gamma_{\text{ch}}^0 \left(\frac{r}{r_s}\right)^g, \quad (14)$$

$$R_{\text{inj}}(r) = R_{\text{inj}}^0 \left(\frac{r}{r_s}\right)^\eta, \quad (15)$$

where γ_{ch}^0 and R_{inj}^0 are the initial value of γ_{ch} and R_{inj} at r_s . The indices g , η describes how the characteristic Lorentz factor and the injection rate evolve with radius r respectively. They are essential to model the rapid rise of the X-ray. In addition, $r_s = 10^{14}$ cm is commonly adopted in all our calculations. We then integrate the flux from a series of rings of which the emitted photons reach the observer at the same time to obtain the light curve of the X-ray flare. In our calculations,

the redshifts of selected GRBs are assumed to be $z = 1$ and the standard Λ CDM universe with $H_0 = 71 \text{ km s}^{-1} \text{ Mpc}^{-1}$, $\Omega_m = 0.27$, and $\Omega_\Lambda = 0.73$ is adopted.

Three GRBs are selected as examples, i.e., GRB 090621A, GRB 121108A, and GRB 140108A, of which the X-ray data show significant rapid rise and steep decay. The numerical results are shown in Figure 1, in comparison with the observed light curve and photon index $\hat{\Gamma}$ ($\hat{\Gamma} = \hat{\beta} + 1$). The corresponding parameters in each case are listed in Table 1. Our results from numerical calculations are in good agreement with the observations. Note that the numerical light curves become steeper than the observed ones at the late stage of the decay phase. However, this deviation does not change our main conclusion. The deviation can be understood in two aspects. There is an obvious turning point in the evolution curve of the observed photon index at the late stage of the decay phase, which strongly indicates that another flare component (or some intrinsic variabilities) should emerge and dominate at that moment. We are only modelling one component of the X-ray light curve, while the observational data do not come purely from one single component. On the other hand, our model is a toy model with some simplified relations, such as Equations (14-15), which makes us unable to model additional variabilities shown in the observational data. If we calculate the flux for the other component and add it to the result, the new total flux would fit the data better.

4. DISCUSSION

In this study, we consider the anisotropy of the synchrotron radiation in the high-latitude emission and apply it to the observed X-ray flares in three GRBs, i.e., GRB 090621A, GRB 121108A, and GRB 140108A. The steep decay phase can be well interpreted by our scenario in which the intrinsic radiation is limb-brightened. Also, the entire temporal, spectral behavior have been modelled using our simplified model. This is the first evidence that intrinsic synchrotron radiation from the emission site of the X-ray flare may be anisotropic.

The anisotropy of the radiation in the co-moving frame is physically supported. In general, the relativistic reconnection sites are expected to be the main sources of non-thermal electrons in the Poynting-flux-dominated flow. Recent particle-in-cell simulations on particle acceleration in the relativistic reconnection current sheet have revealed that the electrons would be efficiently accelerated by the motional electric field when they bounce back and forth within a magnetic island (see Guo et al. 2014, 2015 for details). The acceleration along the motional electric field (perpendicular to the X-line plane of the reconnection) would naturally give a preferable angular distribution for electrons. This preferable angular distribution is consistent with the function $f(\alpha)$ used in our work. Thus the identification of the role the anisotropy plays in the steep decay of X-ray flares would give useful clues for the details of particle acceleration in the emitting region.

It has been proposed that the steep decay of the X-ray flares may be the evidence for the emission site being accelerating. However, in our work, we attribute the steep decay to the anisotropy

of the radiation, rather than the acceleration of the jet. Both mechanisms can explain some current observational features. Observations on the polarisation of X-ray flares may help to identify the prior model since the preferable relative orientation between the \mathbf{B}' field and the electrons moving direction in our model may lead to a polarization degree different from the other model (being prepared). On the other hand, since both mechanisms can coexist naturally in the same frame work (the jet is Poynting-flux dominated), the possibility that they work together within the sample selected can not be neglected. In Uhm & Zhang (2016), they found that the acceleration of the emission region is needed to interpret spectral lags in the prompt emission, but a shallower acceleration index is required, which suggests that the X-ray flare decay may have a contribution from the anisotropic effect. Beniamini & Kumar (2016) suggests that the material producing the X-ray flare may be confined to a jet which is narrow compared to $1/\Gamma$, this provides another possible solution to the steep decay.

An anisotropic minijets model has been invoked to explain the short time-scale variability of the GRB prompt emission (Barniol Duran et al. 2016), in which the radiation is also anisotropic in the co-moving frame. Relevant works show that minijets are essential in defining light curves of the prompt emission (Zhang & Zhang 2014; Deng et al. 2015, 2017). The anisotropic characteristics in the GRB emission mechanism thus seem to be common and need more researches.

We thank the referee, Prof. Pawan Kumar for very valuable suggestions. We also thank Liang Li for helpful discussion. This work is partially supported by the National Basic Research Program (“973” Program) of China (grant No. 2014CB845800) and the National Natural Science Foundation of China (grants No. 11473012 and 11573014). The authors acknowledge support by the Strategic Priority Research Program of the Chinese Academy of Sciences (“Multi-waveband Gravitational Wave Universe” with Grant No. XDB23040000). This work made use of data supplied by the UK Swift Science Data Center at the University of Leicester.

REFERENCES

- Band, D., Matteson, J., Ford, L., et al. 1993, *ApJ*, 413, 281
- Barniol Duran, R., Leng, M., & Giannios, D. 2016, *MNRAS*, 455, L6
- Beloborodov, A. M., Daigne, F., Mochkovitch, R., & Uhm, Z. L. 2011, *MNRAS*, 410, 2422
- Beniamini, P., & Granot, J. 2016, *MNRAS*, 459, 3635
- Beniamini, P., & Kumar, P. 2016, *MNRAS*, 457, L108
- Bromberg, O., & Tchekhovskoy, A. 2016, *MNRAS*, 456, 1739

³This approach was presented in Uhm & Zhang (2016) to model the data for the first time.

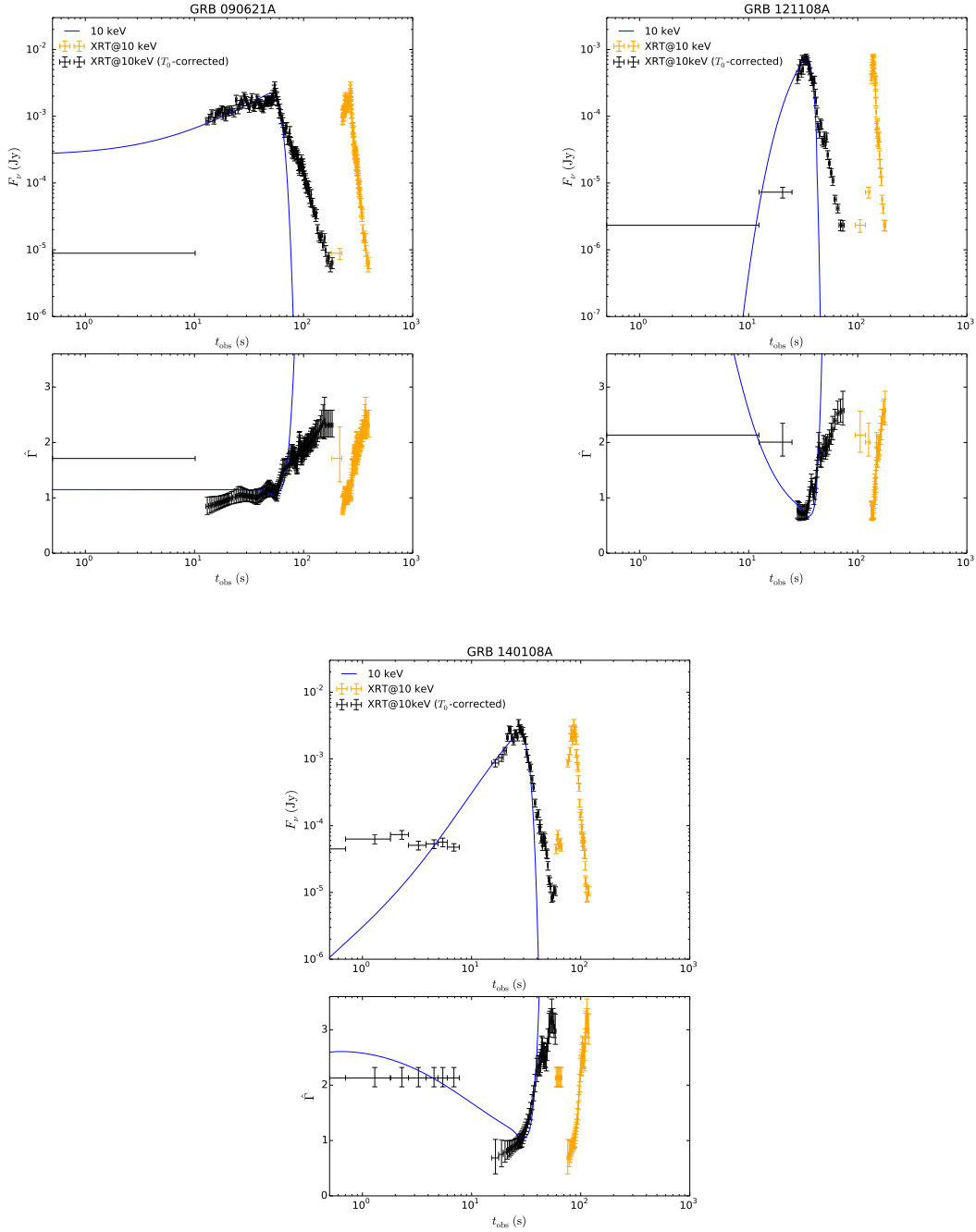


Fig. 1.— Modeling the X-ray flares in GRB 090621A, GRB 121108A and GRB 140108A by using the anisotropic radiation scenario. For each GRB, in the upper panel, the original observed light curve at 10 keV (the orange points) is shown. The black points are the “shifting” version³ of the original data by setting the reference time at T_0 (see details in Section 3) and the model-calculated light curve is presented as a blue line. The lower panel is similar to the upper panel, but presents the corresponding XRT band (0.3–10 keV) photon index.

- Burrows, D. N., Romano, P., Falcone, A., et al. 2005, *Science*, 309, 1833
- Chincarini, G., Moretti, A., Romano, P., et al. 2007, *ApJ*, 671, 1903
- Dai, Z. G., & Gou, L. J. 2001, *ApJ*, 552, 72
- Dai, Z. G., Wang, X. Y., Wu, X. F., & Zhang, B. 2006, *Science*, 311, 1127
- Deng, W., Li, H., Zhang, B., & Li, S. 2015, *ApJ*, 805, 163
- Deng, W., Zhang, B., Li, H., & Stone, J. M. 2017, arXiv:1704.03468
- Dermer, C. D. 2004, *ApJ*, 614, 284
- Gehrels, N., Chincarini, G., Giommi, P., et al. 2004, *ApJ*, 611, 1005
- Giannios, D. 2006, *A&A*, 455, L5
- Granot, J. 2005, *ApJ*, 631, 1022
- Granot, J. 2016, *ApJL*, 816, L20
- Granot, J., Piran, T., & Sari, R. 1999, *ApJ*, 513, 679
- Guo, F., Li, H., Daughton, W., & Liu, Y.-H. 2014, *Physical Review Letters*, 113, 155005
- Guo, F., Liu, Y.-H., Daughton, W., & Li, H. 2015, *ApJ*, 806, 167
- Huang, Y. F., Gou, L. J., Dai, Z. G., & Lu, T. 2000, *ApJ*, 543, 90
- Huang, Y.-F., Lu, Y., Wong, A. Y. L., & Cheng, K. S. 2007, *ChJAA*, 7, 397
- Jia, L.-W., Uhm, Z. L., & Zhang, B. 2016, *ApJS*, 225, 17
- Kumar, P., & Panaitescu, A. 2000, *ApJL*, 541, L51
- Kumar, P., & Zhang, B. 2015, *Phys. Rep.*, 561, 1
- Lazzati, D., & Perna, R. 2007, *MNRAS*, 375, L46
- Liang, E. W., Zhang, B., O’Brien, P. T., et al. 2006, *ApJ*, 646, 351
- Lyubarsky, Y. 2009, *ApJ*, 698, 1570
- Margutti, R., Guidorzi, C., Chincarini, G., et al. 2010, *MNRAS*, 406, 2149
- Maxham, A., & Zhang, B. 2009, *ApJ*, 707, 1623
- Mészáros, P., & Rees, M. J. 1997, *ApJL*, 482, L29
- Moderski, R., Sikora, M., & Bulik, T. 2000, *ApJ*, 529, 151

- Paczynski, B. 1986, *ApJL*, 308, L43
- Perna, R., Armitage, P. J., & Zhang, B. 2006, *ApJL*, 636, L29
- Proga, D., & Zhang, B. 2006, *MNRAS*, 370, L61
- Rees, M. J., & Mészáros, P. 1992, *MNRAS*, 258, 41
- Rybicki, G. B., & Lightman, A. P. 1979, *Radiative Processes in Astrophysics* (New York: Wiley-Interscience)
- Shemi, A., & Piran, T. 1990, *ApJL*, 365, L55
- Uhm, Z. L., & Zhang, B. 2015, *ApJ*, 808, 33
- Uhm, Z. L., & Zhang, B. 2016, *ApJL*, 824, L16
- Uhm, Z. L., & Zhang, B. 2016, *ApJ*, 825, 97
- Waxman, E. 1997, *ApJL*, 491, L19
- Zhang, B., Fan, Y. Z., Dyks, J., et al. 2006, *ApJ*, 642, 354
- Zhang, B., & Yan, H. 2011, *ApJ*, 726, 90
- Zhang, B., & Zhang, B. 2014, *ApJ*, 782, 92

Table 1. Parameters used in the modelling of the X-ray flares of the three GRBs.

Parameters	GRB 090621A	GRB 121108A	GRB 140108A
a	0.15	0.08	0.11
ζ	-0.58	-0.35	-0.48
B_0^\dagger (G)	100.0	100.0	100.0
Γ	30.0	23.0	22.0
γ_{ch}^0 (10^4)	2.4	0.6	1.2
g	0.0	1.35	0.7
η	0.0	0.7	0.0
ΔT (s)	10.0	2.0	6.5
R_{inj}^0 (10^{48} s $^{-1}$)	3.2	3.6	22.0
r_{off} (10^{14} cm)	10.0	3.65	3.3

$^\dagger B_0$ is the strength of the rest frame magnetic field \mathbf{B}' .